
Scalable Computing: Practice and Experience, ISSN 1895-1767, http://www.scpe.org
© 2025 SCPE. Volume 26, Issues 2, pp. 888–898, DOI 10.12694/scpe.v26i2.4057

IMPROVING NODE LOCALIZATION ACCURACY IN WIRELESS SENSOR NETWORKS BASED ON COMPUTER VISION AND DEEP LEARNING OPTIMIZATION

LIANJUN YI *

Abstract. In order to solve the problem of angular effects and reduced positioning accuracy caused by rapid speed changes in position tracking and positioning methods in wireless sensor networks, as well as the difficulty of improving positioning accuracy with a single solution, the author proposes a research on improving node positioning accuracy in wireless sensor networks based on computer vision and deep learning optimization. The author proposes a tracking and localization method using Kalman filtering (KF) and visual assistance on the TI CC2431 ZPS platform. On the basis of normalized cross-correlation, visual assistance calibration technology is used to extract the position of reference nodes as landmarks using visual assistance methods. Then, the KF method is used to calibrate the position estimation, which randomly generates virtual nodes for neural network training. Then, the priority positioning node is located and used as the anchor node for the next positioning, and the wireless loop is used for positioning calculation. The experimental results show that both the TI ZPS method and the KF based method have an estimated position error distance of over 55%, which is less than 2.2m and 1.8m, respectively, The proposed tracking and positioning method has an estimated position error distance of over 55% less than 1.4m. The method proposed by the author effectively avoids uncertainty caused by system errors in actual dynamic environments, reduces angular effects in position estimation systems, and improves positioning accuracy.

Key words: Wireless sensor network, Tracking and positioning, Kalman filtering, Visual assistance, ZPS platform

1. Introduction. With the development of information technology, data is growing at a massive speed, and more and more data is being discovered and utilized. Data that was once unattainable or unused can be collected under the background of new technologies, thus forming the era of big data [1]. Sensors, as an important source of information collection in the physical world, are widely used in various industries. Different sensors have different functions, and a large number of sensors use the same protocol to form a network called Wireless Sensor Networks (WSNs) [2,3]. Wireless sensor networks can achieve functions such as data perception, data collection, and data transmission. Usually, wireless sensors use hardware devices that collect information as wireless sensor nodes, such as smoke alarms, water level monitoring sensors, water quality monitoring sensors, video monitors, etc. These sensors are mainly used to collect certain data. The broad definition of wireless sensors refers to all devices that can provide data, which expands the range of wireless sensors from both ends [4]. In traditional application industries, data collection, data transmission, and other functions can be achieved by installing embedded devices. For example, in traditional washing machines, adding power starters and wireless receiving modules can achieve semi-automatic control. The washing machine can be operated through mobile phones, and shared bicycles can be shared in real-time by adding Bluetooth locks or 4G modules [5]. The emergence of wireless sensor technology has upgraded many functions in traditional industries, and traditional devices are empowered with new functions through new technologies. In the context of new technologies, with the development of 5G and cloud computing, a large number of new products come with the function of implanting wireless sensors. For example, autonomous vehicles are a new device filled with wireless sensors, such as SLAM photodetectors, steering wheel controllers, brake systems, path imaging, etc., all of which collect data through sensors and provide real-time feedback through data transmission. Various wireless sensors are no longer simple single individuals, but they become a collaborative whole. After being hard IPed by intelligent algorithms, sensors can even become execution agencies [6]. Wireless sensors with unlimited types, functions, manufacturers, and regions can form a wireless sensor network within a certain range using the same communication protocol. For example, ZigBee New communication methods such as Lora, NB IoT,

*School of Information Engineering, Gannan University of Science and Technology, Ganzhou, 341000, Jiangxi, China (Corresponding author, 9320240018@gnust.edu.cn)

Sigfox, and WiFi can be embedded in devices through communication modules for self-organizing networks.

2. Literature Review. Numerical optimization is an accurate iterative optimization method, and the quality of the solutions obtained greatly depends on the selection of the initial state [7]. When applied to node localization problems, improvements need to be made based on the inherent properties of the problem itself. For example, Mobile Forest Protection Network (FPWSN) has shown significant advantages in reducing forestry economic losses and improving fire prevention efficiency, Mobile Forest Protection Wireless Sensor Networks (FPWSN) have been widely used in the forest conservation sector. Nevertheless, at the current stage of development, the impact of sensor nodes on the system is frequently overlooked in forest fire prevention and control efforts. Xie, J. et al. devised a novel clustering method tailored for mobile FPWSN termed Boltzmann Adaptive Chaotic Salp Swarm Optimization Clustering (BACSSOC). This innovative approach aims to significantly extend the lifespan of the system, minimize energy usage, and diminish system latency [8]. Jin, Z. et al. explored strategies for deploying sensor nodes to minimize deployment costs while guaranteeing continuous target coverage. They utilized the Confidence Information Coverage (CIC) model to formulate the Minimum Deployment Cost Target Permanent Coverage (CICMTP) problem, with the objective of minimizing the sensor node count needed for deployment [9]. Yu, Q. et al. introduced a framework that integrates wireless sensor networks with the Internet of Things (WSN IoT SEC) for advanced environmental monitoring. The study leverages SEM technology to partition the analysis, exploring individual targets with the aid of detectors, machine learning models, and classifiers. A thorough investigation was undertaken, drawing insights from evaluation results and identified patterns, with a focus on highlighting crucial recommendations and underscoring the importance of SEM analysis [10].

The author proposes a position tracking system combined with visual assistance methods in the WSN environment, with the aim of exploring how to improve the corner effect caused by the tracking system. Compared to traditional position estimation, based on normalized cross correlation, the visual assistance method of the NCC method detects landmark positions as calibration, alleviating the angular effects caused by filtering and tracking techniques. More accurate position estimation was obtained in a static WSN environment.

3. Research Methods.

3.1. Basic knowledge.

3.1.1. State and observation equations. In a state-space representation of a dynamic system, if the system is described by a probability density, the state equation of the system measured by MT at time k is given by the following mathematical model 3.1:

$$x_{\lambda+1} = fun_x(x_k, u_K) \leftrightarrow f(x_{k+1}|x_k) \tag{3.1}$$

The observation equation is as follows 3.2:

$$z_k = fun_z(x_k, \epsilon_k) \leftrightarrow h(z_k|x_k) \tag{3.2}$$

Among them,x_k,$fun_k()$,u_k,z_k,$fun_z()$ and ϵ_k are respectively state vectors, transformation equations, process noise with a known distribution, observation vectors, observation equations, and observation noise with a known distribution. The mathematical model and measurement of linear dynamic systems are represented by the following equations 3.3 and 3.4:

$$x_{k+1} = \Phi_k x_k + u_k, u_k \sim N(0, Q_k) \tag{3.3}$$

$$E\{u_n, u_k^T\} = \begin{cases} Q_k, n = k \\ 0, n \neq k \end{cases} = \delta(k-n)Q_k \tag{3.4}$$

The observation equation is as follows 3.5,3.6:

$$z_k = H_k x_k + \epsilon_k, \epsilon \sim N(0, R_k) \tag{3.5}$$

$$E\{\epsilon_n, \epsilon_k^T\} = \begin{cases} R_k, n = k \\ 0, n \neq k \end{cases} = \delta(k-n)R_k \tag{3.6}$$

Among them, x_k,Φ_k,$u_k$and Q_k are the state matrix, state transition matrix, model noise matrix, and model noise covariance matrix, respectively [11,12]. u_k and ϵ_k is a Gaussian vector that is independent of the zero mean of the corresponding covariance matrices Q_k and R_k.

3.1.2. Kalman filtering. Assuming that vector $x = [x_1, \cdots, x_n]^T$ is composed of independent components, $i = 1, \cdots, n$. The PDF of x consists of independent PDFs of $x_1, \cdots, x_n$. $N(x; m, P)$ is The Gaussian density of n-dimensional vectors, the n-dimensional Gaussian density function is defined as follows 3.7:

$$N(x; m, P) \triangleq |2\pi P|^{-1/2} exp\{(-\frac{1}{2}(x-m)^T P^{-1}(x-m))\} \tag{3.7}$$

Among them, x, m, P are parameters, mean, and covariance, respectively. At time $t = t_k$, the vector $x(t)$ value is x_k. At time $t = t_k$, vector $x(t)$ gives the estimated value $x_{k|j}$ at time $t = t_j$ is represented by double subscripts [13].

(1) Prediction stage (time update stage). From From k to k+1, the state prediction and prediction error covariance are calculated using the following equations 3.8, 3.9, and 3.10:

$$\widetilde{x_{k+1}} = \phi_k \hat{x_k} \tag{3.8}$$

$$\widetilde{P_{k+1}} = \Phi_k \hat{P_k} \Phi_k^T + Q_k \tag{3.9}$$

$$\hat{P_k} = \{\hat{e_k} \hat{e_k}\}, \widetilde{P_k} = E\{\tilde{e_k} \tilde{e_k}^T\} \tag{3.10}$$

Among them, $e_{kj} \triangleq x_{k|j} - x_k, e_{k|k} \triangleq \widehat{x_k} - x_k = \hat{e_k}, e_{k|k-1} \triangleq \widetilde{x_k} - x_k = \tilde{e_k} \circ \widehat{x_k}$, $\widetilde{x_k}, e_{k|j}, \hat{e_k}, \tilde{e_k}$ are state estimation matrix, the status forecast matrix, the status error matrix, the estimated error matrix, and the forecast error matrix are respectively[14].

(2) Innovation stage. The calculation formula for the innovation stage is as follows 3.11,3.12:

$$zz_k = z_k - H_k \tilde{x_k} \tag{3.11}$$

$$K_k = \tilde{P_k} H_k^T [H_k, \tilde{P} H_k^T + R_k]^{-1} \tag{3.12}$$

Among them, zz_k and K_k are the innovation matrix and the Kalman gain matrix, respectively.

(3) Correction phase. The state estimation and the update of the estimation error covariance are as follows 3.13,3.14:

$$\hat{x_k} = \tilde{x_k} + K_k zz_k \tag{3.13}$$

$$\hat{P_k} = [I - K_k H_k] \tilde{P_k} \tag{3.14}$$

Among them, I represents the identity matrix.

3.1.3. Normalized cross-correlation. To determine a reference node as a route marker (RN) the author combined a pattern recognition method with RN (ID) for estimating position calibration [15]. It is well-known that NCC is one of the most basic area-based matching techniques. The NCC scheme is extensively utilized in image processing applications, as it can mitigate brightness discrepancies between images and templates resulting from varying lighting conditions. The NCC equations used by the author are 3.15, 3.16, 3.17, 3.18, 3.19, and 3.20:

$$G_T = \frac{\sum_{i=1}^{n} \sum_{j=1}^{m} G_T(x_i, y_j)}{n \cdot m} \tag{3.15}$$

$$G_S = \frac{\sum_{i=1}^{n}\sum_{j=1}^{m} G_S(x_i, y_j)}{n \cdot m} \tag{3.16}$$

$$\sigma_T = \sqrt{\frac{\sum_{i=1}^{n}\sum_{j=1}^{m}(G_T(x_i, y_j) - G_T)^2}{n \cdot m - 1}} \tag{3.17}$$

$$\sigma_S = \sqrt{\frac{\sum_{i=1}^{n}\sum_{j=1}^{m}(G_S(x_i, y_j) - G_S)^2}{n \cdot m - 1}} \tag{3.18}$$

$$\sigma_T S = \frac{\sum_{i=1}^{n}\sum_{j=1}^{m}[(G_T(x_i, y_j) - G_T) \cdot (G_S(x_i, y_j) - G_S)]}{n \cdot m - 1} \tag{3.19}$$

$$r = \frac{\sigma_{TS}}{\sigma_T \sigma_S} \tag{3.20}$$

Among them, $G_T(x, y)$ and $G_S(x, y)$ are grayscale images of the target window and search window, respectively; G_T and G_S are the grayscale values of the target window and search window, respectively; m and n are the number of rows and columns, respectively.

3.1.4. ZigBee positioning system. The ZigBee network, which is IEEE 802.15.4, is designed to facilitate the communication of information at a low, low-power and cost-free time while maintaining the route. In Figure 1, a fundamental location system utilizing a ZigBee network is shown, wherein the Received Signal Strength Indicator (RSSI) is used to measure the power of a received wireless signal. The ZigBee Positioning System (ZPS) includes three kinds of nodes, namely, an index, a RN, and a BN. The coordinator is attached directly to the computer as shown in Figure 1. The RNs, which are located in a known position, send to the BN their equipment ID and its coordinates. Each stationary RN is located at a predefined location. A BN node collects a signal from an RN in accordance with an RSSI value for an RN. When a BN receives a signal from an RN, it identifies a distance between a BN and an individual RN by means of the RSSI sample collected together with a route loss model. The location of the BN is then computed according to the RNN coordinates. Eventually, the BN's estimated location is transferred through a WSN to a Location-Based Services (LBS) app.

3.2. Proposed algorithm. The method for measuring uncertainty in WSN utilizes the widely-used commercial system ZPS, which is based on the CC2431 positioning engine developed by Texas Instruments (TI). Detailed technical information about the TI CC2431 can be found at http://www.ti.com/product/cc2431. The TI CC2431 is a hardware localization engine specifically designed for low-power local area network (ZigBee) applications within WSN [16-18]. In Ad Hoc wireless networks, it is used to evaluate BN position estimation based on RSSI values (from RN, obtained by centralized computing methods). According to the RSSI value, The TI CC2431 positioning engine independently outputs (X , Y) Coordinates. The author focuses on having independent (X , Y) The localization and tracking scheme for the group.

3.2.1. Formulaization of problems. To enhance the accuracy of position tracking, the tracking method can be reformulated as a filtering problem. This involves integrating Kalman Filter (KF) based techniques into position estimation systems using tracking algorithms to enhance the accuracy of the positioning system. While the state and measurement models typically operate within two-dimensional linear Gaussian systems, extending the approach to three-dimensional models is straightforward within the framework of filtering methods. The two-dimensional model vector $x_k = [x_{1,k}, x_{2,k}, \dot{x}_{1,k}, \dot{x}_{2,k}]^T$ represents the state of MT at time k, where, $x_{1,k}$ and $x_{2,k}$ respectively represent X , Y coordinate. $\dot{x}_{1,k} = s_{1,k}$ and $\dot{x}_{2,k} = s_{2,k}$ are represent the velocities in the X and Y directions, respectively [19]. The speed model for the MT is founded on speed noise. The two-dimensional model of the MT characterizes its movement and observed position by incorporating random elements, and the

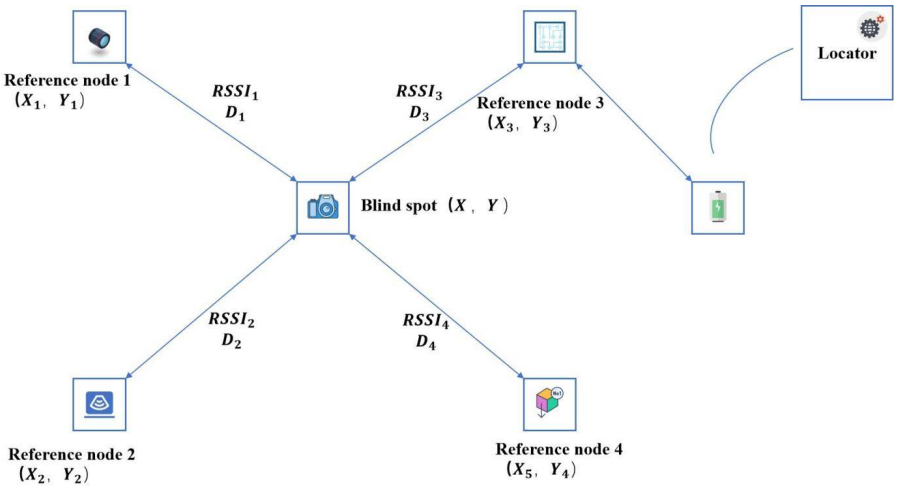

Fig. 3.1: Simple positioning system based on ZigBee network

formula for calculation is provided in equations 3.21 and 3.22.

$$\begin{bmatrix} x_{1,k+1} \\ x_{2,k+1} \\ \dot{x}_{1,k+1} \\ \dot{x}_{2,k+1} \end{bmatrix} = \begin{bmatrix} x_{1,k+1} \\ x_{2,k+1} \\ s_{1,k+1} \\ s_{2,k+1} \end{bmatrix} = \begin{bmatrix} 1 & 0 & \Delta_k & 0 \\ 0 & 1 & 0 & \Delta_k \\ 0 & 0 & 1 & 0 \\ 0 & 0 & 0 & 1 \end{bmatrix} = \begin{bmatrix} x_{1,k+1} \\ x_{2,k+1} \\ \dot{x}_{1,k+1} \\ \dot{x}_{2,k+1} \end{bmatrix} = \begin{bmatrix} u_{1,k+1} \\ u_{2,k+1} \\ u_{3,k+1} \\ u_{4,k+1} \end{bmatrix} \tag{3.21}$$

$$\begin{bmatrix} z_{1,k} \\ z_{2,k} \end{bmatrix} = \begin{bmatrix} 1 & 0 & 0 & 0 \\ 0 & 1 & 0 & 0 \end{bmatrix} = \begin{bmatrix} x_{1,k+1} \\ x_{2,k+1} \\ \dot{x}_{1,k+1} \\ \dot{x}_{2,k+1} \end{bmatrix} + \begin{bmatrix} \epsilon_{1,k} \\ \epsilon_{2,k} \end{bmatrix} \tag{3.22}$$

Among them, Δ_k is the measurement period between k and k+1. The difference between equations 3.3 and 3.5 and equations 3.21 and 3.22 can be represented by $u_k = [u_{1,k}, u_{2,}, u_{3,k}, u_{4,k}]^T$ for process noise; $z_k = [z_{1,k}, z_{2,k}]$ and $\epsilon_k = [\epsilon_{1,k}, \epsilon_{2,k}]$ represents respectively Observation information and measurement noise of MT at time k [20].

3.2.2. Visual assisted position estimation. In the WSN environment, signals are affected by reflection, diffraction, scattering, and attenuation effects during propagation, and the instability of RSSI values can also affect positioning accuracy. The signal feedback of the TI CC2431 positioning engine is greatly affected by RSSI information, which can reduce positioning accuracy [21]. To enhance positioning accuracy, a technique leveraging auxiliary markers is employed to counteract angular distortions caused by filtering and tracking methods in dynamic, changing environmental conditions. This method facilitates calibration and positioning based on sensor landmark positions. RN landmarks are extracted from video features using the NCC method for precise position estimation. Moreover, to conserve energy and extend the lifespan of intelligent mobile terminals utilizing the NCC method for position estimation, this approach enables the simultaneous operation of two modes based on a shared threshold: Sleep mode and activity mode. The threshold, derived from RSSI and ZPS testing platforms, determines whether the visual assistance algorithm remains in active mode based on the detected RSSI level [22]. As the BN nears the RN, the video camera of the intelligent mobile terminal initiates path recording and subsequently identifies landmarks using the NCC method. Conversely, when the RSSI surpasses the threshold, the visual assistance algorithm transitions into sleep mode, halting path recording by the video camera. Figure 3.2 illustrates an instance of the visual assistance scheme utilizing the NCC method. Experimental findings demonstrate the efficacy of the NCC method in accurately extracting RN from video features as the correct landmark.

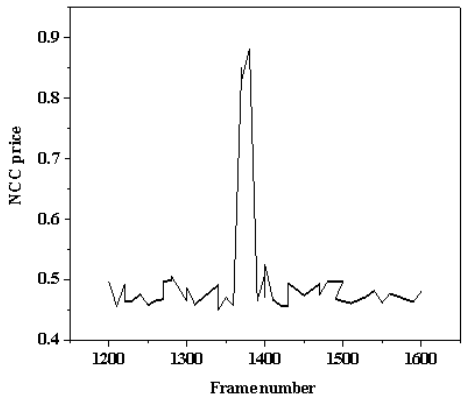

Fig. 3.2: Example of extracting RN as a landmark

3.3. Analysis of RBF-HOP localization algorithm.

3.3.1. The process of positioning algorithm. The positioning algorithm mode adopted by the author is centralized. In this model, the key point of this model is to transmit the hop number of the WSN to one of the WSN's non-known nodes and its anchor points, and then analyzes and determines the specific positions of each unknown node through this processing center. This approach doesn't demand high hardware specifications for wireless sensors and concurrently lowers the energy consumption of wireless sensor node processing during positioning operations. However, this computational technique necessitates awareness of the minimum hop count value between nodes within the wireless sensor network. The positioning calculation process mainly includes the following points: Firstly, adjust the hop count of each anchor node to 0, that is, adjust it to the initialization position, so that further calculations can be carried out; Secondly, once an anchor node has been identified, it will be able to transmit a particular position message to the adjacent nodes; Thirdly, for each neighboring node that receives information packets, the hop count should be updated to the anchor node's hop count, and then an additional 1 should be added to this hop count. After that, the information packets should be propagated to the next adjacent node; Upon receiving hop count information from the preceding node, the subsequent node adjusts its hop count to ensure that each node's hop count reaches the minimum value. Then, the next hop count information is propagated to other nodes; The fifth step is to repeatedly update the node hop count operation until the node hop count information no longer changes [23].

For instance, if the sensor has if the whole WSN has N nodes, and there are M anchor nodes ($m \leq$), then Among m anchor nodes may be determined to be n, the planar position coordinates of the t-th node can be represented as $m_t = (x_t, y_t)$. In the process of calculating the minimum hop count of an unknown node, the hop count information is directly sent to the service processing center, and the information of that node is recorded and processed. Randomly generate several virtual nodes in a wireless sensor network, and number them in order, counting them as 1, 2, 3, etc. The node plane coordinates are marked according to the numbers. Then, using the known radiation radius of the sensor nodes, combined with the hop calculation process, calculate the specific hop count value from each virtual node to the anchor node. Record their hop count in a matrix format, and input the matrix hop count into the input layer of the RBF neural network for training, after the training is completed, its corresponding expected output value is the actual coordinates calculated by the node [24]. Moreover, it is also possible to take the hop count of the anchor point as a training input in RBF net and compute the coordinate of the anchor point.

3.3.2. Localization of Unknown Nodes. The RBF neural network has memory after being trained with input from nodes, and can use its memory function to simulate the hop characteristics and position relationships in wireless sensor networks. There is a matrix hop count between each unknown node and the

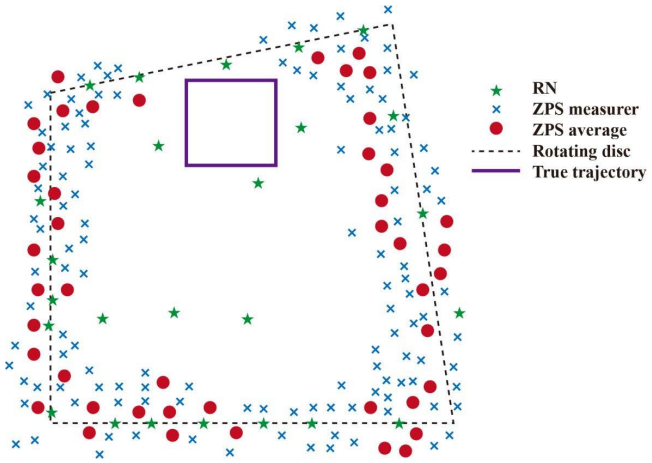

Fig. 4.1: Position estimation results of MT (BN) moving along the test path in the TI ZPS platform

anchor node, so in the process of selecting priority positioning nodes, the hop count matrix can also be selected. For example, when the hop matrix of the anchor node is $nm_t = [h_{t1}h_{t2}h_{t3}\cdots h_{tm}]$ and the hop matrix is input into the trained RBF neural network, there are: Nodes the coordinates of n_t are (x_t, y_t). The localization algorithm process for its unknown nodes is as follows: firstly, randomly generate several unknown nodes and anchor nodes, assuming that the number of unknown nodes is n and the number of anchor nodes is m; The second is to randomly generate several virtual nodes, assuming that the number of virtual nodes is denoted as v; Thirdly, utilizing virtual nodes to train RBF neural networks; The fourth is to select the optimal localization node from several unknown nodes, and then input it into the network for localization; The fifth is to use a series of nodes with known positions as anchor nodes; The sixth step is to locate the loop nodes until all unknown nodes are accurately located.

4. Result analysis.

4.1. Experimental setup. The experimental platform is located on the top floor of the Remote Sensing Research Center, with a sampling distance of 1 meter, RNs (1-26) are widely distributed on rooftops, with 15 RNs distributed in the closed-loop path of sampling locations. In addition, in order to obtain the optimal and precise position of the sampling points, the isotropic radiation characteristics of the antenna are enhanced in the positioning system. Hence, to enhance the accuracy of RSSI measurements, a straightforward antenna radiation mapping approach was employed. This involved positioning the BN on a turntable capable of rotating to ensure that the RN's radiation antenna consistently faced north, west, south, and east. RSSI information was then recorded at various distances between the RN and BN (ranging from 1 to 10 meters) in each direction. This data was subsequently input into the TI CC2431 system to estimate the location. Nonetheless, within wireless network systems, positional errors depend on the information environment RN deployment mode and density. Usually, the more RNs available within the same given area, the more accurate the localization.

4.2. ZigBee positioning system. In wireless network systems, ZPS uses the RSSI value of the TI CC2431 positioning engine for localization. This experiment used a visual assistance scheme combined with TI CC2431 ZPS platform for position estimation and trajectory tracking. As the MT traverses the designated testing path, the experimental outcomes of position estimation based on the TIZPS platform are depicted in Figure 4.1. In this representation, the symbol "x" denotes the estimated position, representing the ZPS measurements. To validate the proposed scheme's experimental findings, Figure 4.1 showcases the corresponding positional parameters associated with the estimated results. It is assumed, without loss of generality, that the MT in equation 3.21 maintains a stable state, with the measurement period (sample time) between k and k+1 set to 1 second. Additionally, Figure 4.1 illustrates the visual position as defined in equation 3.22.

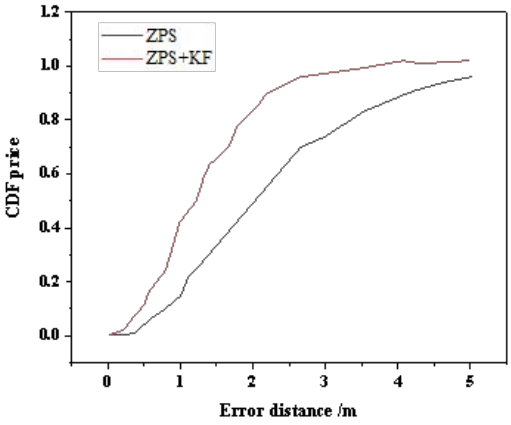

Fig. 4.2: CDPF of error distance for ZPS (observation) and KF based tracking methods

4.3. Position estimation based on Kalman filtering. Figure 4.2 shows the results of the simulation for the location estimation in a tracking system. The results show that the location precision obtained by this method is superior to that of nontracking. In particular, Kalman Filter (KF), being based on the optimum tracking of a Gauss model, usually produces the best linear estimation in the mean square error. Therefore, it is possible to consider the location precision in the KF tracing scheme as an upper limit of the CDF (CDF) for location estimation under Gauss circumstance [25]. The results show that the TI ZPS scheme has an estimated position error distance of over 56% less than 2.2 meters; With the KF-based approach, over 55% of estimated position error distances fall below 1.8 meters. The precision of KF tracing is better than that of ZPS nontracking, as demonstrated by the experiments in Figure 4.3. Notably, the KF method's hallmark is its recursive minimum mean square error state algorithm. Consequently, the position error observed in the KF tracking algorithm can serve as the upper bound for the cumulative distribution function (CDF) across various position estimation methods.

4.4. Visual assisted position estimation. Based on the experience values provided by TI company, The TI CC2431 positioning engine sets the threshold for RSSI in the ZPS platform to 60. When the Received Signal Strength Indicator (RSSI) exceeds 60, the visual assistance algorithm shifts into active mode, initiating landmark detection via the NCC method. Figure 4.3 showcases the experimental outcomes of a visual assistance scheme utilizing the NCC method. The 'r' value denotes the most probable video frame when encountering landmarks. Drawing insights from the experimental findings depicted in Figure 4.3, When the r value is around 0.6, most high peaks can be clearly distinguished, and the optimal value is estimated to be 0.62. Therefore, in the NCC method The threshold for r value is set to 0.62, at this point, RN can accurately detect landmarks and achieve good results. The results indicate that over 55% of estimated position error distances are less than 1.4 meters. The experimental results in Figure 4.3 show that the proposed scheme has better positioning accuracy than non visual assisted methods. Visual assistance methods can provide high-precision positioning estimation and trajectory tracking. The combination of NCC based visual technology and KF based algorithms shows that the tracking scheme proposed by the author results in close proximity to MT's tracking and positioning. Therefore, the visual assistance method based on NCC method can effectively solve and overcome the impact of dynamic time changing environments on the path. Due to the suitability of this position tracking platform for various practical applications.

In scenarios where GPS signals are unavailable, such as indoors or in outdoor environments with signal blockages, continuous real-time position tracking becomes challenging. Hence, integrating various strategies into position estimation systems becomes crucial for enhancing positioning accuracy. Combining visual assistance

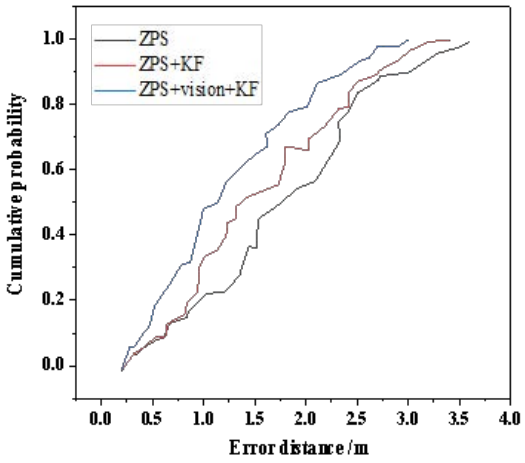

Fig. 4.3: Comparison of ZPS (observation), KF based and visually assisted KF trajectory tracking methods

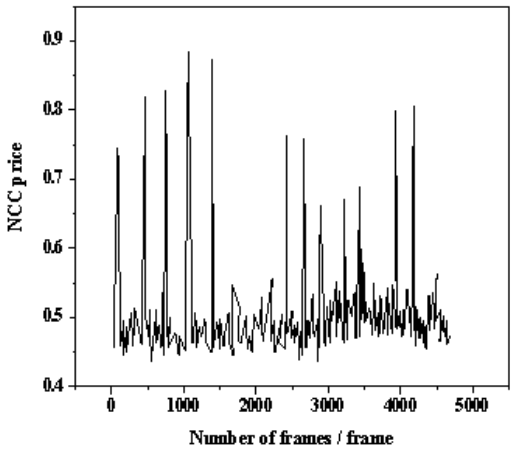

Fig. 4.4: RN image matching results based on NCC method when MT (BN) moves along the test path

methods with position tracking technology forms a pivotal component, acting as a fuse within multi-sensor positioning systems. This fusion approach significantly improves the accuracy of MT position estimation in Location-Based Services (LBS) applications.

5. Conclusion. The author proposes a visual assisted method for position estimation and trajectory tracking based on the WSN environment. In the ZPS platform, based on the KF method, MT can accurately track position changes and improve positioning accuracy. In addition, The NCC process matches RN images and extracts RN as landmarks from video features. In a stable operational setting, the KF tracking scheme leverages RN information to refine position estimation, effectively mitigating angular distortions. Experimental findings underscore the superior accuracy of the proposed scheme over non-tracking and non-visual assistance

methods. Notably, more than 55% of estimated positions exhibit error distances of less than 1.4 meters. By integrating visual assistance and KF tracking methodologies within the ZPS platform of WSN, the author's proposed positioning and tracking platform offers significant enhancements compared to standalone approaches, which has strong advantages for various LBS applications. The author only considered static WSN, mainly to facilitate formal description of the problem. In the future, more challenging dynamic WSN tracking and localization problems will be considered.

6. Acknowledgement. Science and Technology Project of Jiangxi Provincial Department of Education (No.GJJ2204405)

REFERENCES

[1] Kim, T., Vecchietti, L. F., Choi, K., Lee, S., & Har, D. (2020). Machine learning for advanced wireless sensor networks: A review. IEEE Sensors Journal, 21(11), 12379-12397.
[2] Kumar, M., Mukherjee, P., Verma, K., Verma, S., & Rawat, D. B. (2021). Improved deep convolutional neural network based malicious node detection and energy-efficient data transmission in wireless sensor networks. IEEE Transactions on Network Science and Engineering, 9(5), 3272-3281.
[3] Nurlan, Z., Zhukabayeva, T., Othman, M., Adamova, A., & Zhakiyev, N. (2021). Wireless sensor network as a mesh: Vision and challenges. IEEE Access, 10, 46-67.
[4] Lin, C., Han, G., Qi, X., Du, J., Xu, T., & Martínez-García, M. (2020). Energy-optimal data collection for unmanned aerial vehicle-aided industrial wireless sensor network-based agricultural monitoring system: A clustering compressed sampling approach. IEEE Transactions on Industrial Informatics, 17(6), 4411-4420.
[5] Ouyang, A., Lu, Y., Liu, Y., Wu, M., & Peng, X. (2021). An improved adaptive genetic algorithm based on DV-Hop for locating nodes in wireless sensor networks. Neurocomputing, 458, 500-510.
[6] Safaldin, M., Otair, M., & Abualigah, L. (2021). Improved binary gray wolf optimizer and SVM for intrusion detection system in wireless sensor networks. Journal of ambient intelligence and humanized computing, 12, 1559-1576.
[7] Dao, T. K., Nguyen, T. D., & Nguyen, V. T. (2023). An improved honey badger algorithm for coverage optimization in wireless sensor network. Journal of Internet Technology, 24(2), 363-377.
[8] Xie, J., Zhang, M., Jin, B., Zhai, J., Wang, Z., & Xiao, J., et al. (2023). Bacssoc: a novel clustering method for mobile forest protection using wireless sensor network with lower energy consumption and lower latency. Simulation modelling practice and theory: International journal of the Federation of European Simulation Societies, 114(3), 2017-2042.
[9] Jin, Z., Geng, Y., Zhu, C., Xia, Y., Deng, X., & Yi, L., et al. (2024). Deployment optimization for target perpetual coverage in energy harvesting wireless sensor network. Digital Communications and Networks, 10(2), 498-508.
[10] Yu, Q., Xiong, F., & Wang, Y. (2022). Integration of wireless sensor network and iot for smart environment monitoring system. Journal of Interconnection Networks, 22(Supp02), 11975-12023.
[11] Cui, Y., Zhang, L., Hou, Y., & Tian, G. (2021). Design of intelligent home pension service platform based on machine learning and wireless sensor network. Journal of Intelligent & Fuzzy Systems, 40(2), 2529-2540.
[12] Kunhoth, J., Karkar, A., Al-Maadeed, S., & Al-Ali, A. (2020). Indoor positioning and wayfinding systems: a survey. Human-centric Computing and Information Sciences, 10, 1-41.
[13] Liu, F., Liu, J., Yin, Y., Wang, W., Hu, D., Chen, P., & Niu, Q. (2020). Survey on WiFi-based indoor positioning techniques. IET communications, 14(9), 1372-1383.
[14] Farahsari, P. S., Farahzadi, A., Rezazadeh, J., & Bagheri, A. (2022). A survey on indoor positioning systems for IoT-based applications. IEEE Internet of Things Journal, 9(10), 7680-7699.
[15] Holmqvist, K., Örbom, S. L., Hooge, I. T., Niehorster, D. C., Alexander, R. G., Andersson, R., ... & Hessels, R. S. (2023). RETRACTED ARTICLE: Eye tracking: empirical foundations for a minimal reporting guideline. Behavior research methods, 55(1), 364-416.
[16] Liu, S., Liu, D., Muhammad, K., & Ding, W. (2021). Effective template update mechanism in visual tracking with background clutter. Neurocomputing, 458, 615-625.
[17] Chen, X., Li, Z., Yang, Y., Qi, L., & Ke, R. (2020). High-resolution vehicle trajectory extraction and denoising from aerial videos. IEEE Transactions on Intelligent Transportation Systems, 22(5), 3190-3202.
[18] Li, Y., Zhuang, Y., Hu, X., Gao, Z., Hu, J., Chen, L., ... & El-Sheimy, N. (2020). Toward location-enabled IoT (LE-IoT): IoT positioning techniques, error sources, and error mitigation. IEEE Internet of Things Journal, 8(6), 4035-4062.
[19] Kuvondikovna, K. S., & Hakima, B. (2024). Designing Visual Aid. European Journal of Higher Education and Academic Advancement, 1(2), 165-167.
[20] Mbanda, N., Dada, S., Bastable, K., & Ingalill, G. B. (2021). A sco** review of the use of visual aids in health education materials for persons with low-literacy levels. Patient education and counseling, 104(5), 998-1017.
[21] Khan, M. A., Paul, P., Rashid, M., Hossain, M., & Ahad, M. A. R. (2020). An AI-based visual aid with integrated reading assistant for the completely blind. IEEE Transactions on Human-Machine Systems, 50(6), 507-517.
[22] Al Aqad, M. H., Al-Saggaf, M. A., & Muthmainnah, M. (2021). The impact of audio-visual aids on learning English among MSU third-year students. ENGLISH FRANCA: Academic Journal of English Language and Education, 5(2), 201-214.
[23] Martiniello, N., Eisenbarth, W., Lehane, C., Johnson, A., & Wittich, W. (2022). Exploring the use of smartphones and tablets

among people with visual impairments: Are mainstream devices replacing the use of traditional visual aids?. Assistive Technology, 34(1), 34-45.
[24] Sokhiba, R. (2024). EFFECTIVENESS OF VISUAL AIDS IN TEACHING LANGUAGE. Journal of new century innovations, 51(1), 93-96.
[25] Chiekezie, P. N., & Inyang, M. J. P. (2021). The significance of audio-visual aids in teaching of English vocabulary. GNOSI: An Interdisciplinary Journal of Human Theory and Praxis, 4(2), 54-70.

Edited by: Hailong Li
Special issue on: Deep Learning in Healthcare
Received: May 29, 2024
Accepted: Jul 13, 2024